Changes in the Local Structure of $LiMg_yNi_{0.5-y}Mn_{1.5}O_4$ Electrode Materials during Lithium Extraction

R. Alcántara, M. Jaraba, P. Lavela, and J. L. Tirado*

Laboratorio de Quimica Inorgánica, Edificio C3, Primera Planta, Campus de Rabanales, Facultad de Ciencias, Universidad de Córdoba, 14071 Córdoba, Spain

E. Zhecheva and R. Stoyanova

Institute of General and Inorganic Chemistry, Bulgarian Academy of Sciences, 1113 Sofia, Bulgaria

Received December 23, 2003. Revised Manuscript Received February 17, 2004

The effects of composition and preparation temperature on the structure of $LiMg_yNi_{0.5-y}Mn_{1.5}O_4$ ($y = 0$, 0.25, 0.5) compounds are studied by EPR, FTIR, X-ray, and neutron diffraction. For $y \geq 0.25$, cation ordering in a $P4_332$ superstructure takes place on increasing the annealing temperature from 450 to 750 °C. In contrast, a loss of octahedral cation ordering and partial reduction of transition metals are found for $LiNi_{0.5}Mn_{1.5}O_4$ when preparation temperature increases from 700 to 800 °C. The EPR behavior of $LiMg_{0.5}Mn_{1.5}O_4$ is determined from localized Mn^{4+} ions, whereas residual antiferromagnetic correlations between Ni^{2+} and Mn^{4+} ions give rise to strong resonance absorption for $LiNi_{0.5}Mn_{1.5}O_4$. The magnetic dilution of the Ni^{2+} sublattice by Mg^{2+} or Mg^{2+}/Ni^{2+} causes strong changes in an apparent *g*-factor, whereas the line width undergoes little changes. When $LiMg_yNi_{0.5-y}Mn_{1.5}O_4$ oxides are used as positive electrode materials in test lithium anode cells, the capacity in the 5-V region decreases with decreasing Ni content. Nevertheless, cycling in the 3-V region showed a net improvement on increasing Mg content. Lithium extraction from $LiNi_{0.5}Mn_{1.5}O_4$ (up to 70%) leads to a loss of intensity in the EPR signal as a consequence of the oxidation of paramagnetic Ni^{2+} to diamagnetic Ni^{4+} without significant changes in local environment of Mn^{4+}. For fully delithiated $Li_{1-x}Ni_{0.5}Mn_{1.5}O_4$ oxide, the EPR spectrum from localized Mn^{4+} ions is observed, indicating an exhaustion of paramagnetic Ni^{2+} ions in the vicinity of Mn^{4+} ions.

Introduction

The crystallographic and magnetic structure of the spinel compound $LiNi_{0.5}Mn_{1.5}O_4$ has attracted the interest of different researchers since the early work by Blasse in 1966.[1] Preudhomme[2] ascribed the complexity of the IR spectra and the analogy between the spectra of $LiNi_{0.5}Mn_{1.5}O_4$ and $LiMg_{0.5}Mn_{1.5}O_4$ to the existence of an ordered variety in the former compound with 1:3 octahedral order. In the 1990s, Gryffroy et al.[3,4] examined the crystal structure of $LiNi_{0.5}Mn_{1.5}O_4$ by X-ray and neutron diffraction, and described a $P4_332$ superstructure, similar to that previously found for $LiFe_5O_8$.[5] More recently, Ooms et al.[6] and Strobel et al.[7] confirmed the $P4_332$ superstructure in other $LiNi_{0.5}Mn_{1.5}O_4$ preparations. Similarly,[8,9] the $Fd3m$ space group was found to describe adequately the neutron diffraction data of some preparations of this composition. From these studies, it is clear that the preparation conditions should play a major role in the cation ordering process. However, a detailed description of the effects of preparation on the crystalline and local structures is needed.

Besides these studies, the interest in $LiNi_{0.5}Mn_{1.5}O_4$ increased substantially with the use of $LiMn_2O_4$ spinel as the positive electrode of lithium cells. Thus, Amine et al.[10] found that $LiNi_{0.5}Mn_{1.5}O_4$ prepared by sol−gel technique intercalates lithium at 3 V, without Jahn−Teller distortion, and has a high discharge capacity and good reversibility. When $LiNi_{0.5}Mn_{1.5}O_4$ is prepared by solid-state reaction, two-phase intercalation reaction in the 3-V region has been found and electrochemical cycleability does not show any improvement.[11] From the electrochemical point of view, a good reversibility of Li extraction/insertion in the 3-V region has been found for highly crystallized $LiNi_{0.5}Mn_{1.5}O_4$ oxides only.[12,13]

* To whom correspondence should be addressed. Phone: +34 957 218637. E-mail: iq1ticoj@uco.es.

(1) Blasse, G. *J. Phys. Chem. Solids* **1966**, *27*, 383.
(2) Preudhomme, J. *Ann. Chim.* **1974**, *9*, 31.
(3) Gryffroy, D.; Vandenberghe, R. E.; Legrand, E. *Mater. Sci. Forum* **1991**, *79−82*, 785.
(4) Gryffroy, D.; Vandenberghe, R. E. *J. Phys. Chem. Solids* **1992**, *53*, 777.
(5) Braun, P. B. *Nature* **1952**, *4339*, 1123.
(6) Ooms, F. G. B.; Kelder, E. M.; Schoonman, J.; Wagemaker, M.; Mulder, F. M. *Solid State Ionics* **2002**, *152−153*, 143.
(7) Strobel, P.; Ibarra-Palos, A.; Anne, M.; Poinsignon, C.; Crisci, A. *Solid State Sci.* **2003**, *5*, 1009.
(8) Branford, W.; Green, M. A.; Neumann, D. A. *Chem. Mater.* **2002**, *14*, 1649.
(9) Alcántara, R.; Jaraba, M.; Lavela, P.; Tirado, J. L.; Biensan, Ph.; de Guibert, A.; Jordy, C.; Peres, J. P. *Chem. Mater.* **2003**, *15*, 2376.
(10) Amine, K.; Tukamoto, H.; Yasuda, H.; Fujita, Y. *J. Electrochem. Soc.* **1996**, *143*, 1607.
(11) Strobel, P.; Ibarra Palas, A.; Anne, M.; Le Cras, F. *J. Mater. Chem.* **2000**, *10*, 429.
(12) Okada, M.; Lee, Y.-S.; Yoshio, M. *J. Power Sources* **2000**, *90*, 196.

10.1021/cm035369c CCC: $27.50
Published on Web 03/23/2004

Later,[14−20] it was found that electrodes with this material could be charged, giving a significant reversible capacity at ca. 4.7 V. The optimization of the high-voltage electrode material has been the subject of different recent studies.[16−19] Among other improvements, the positive effect of doping with Mg[7] and Ti[9] has been demonstrated. The presence of Mg or Ti in the structure of $LiNi_{0.5}Mn_{1.5}O_4$ was shown to have very different consequences.[3] Thus, for Ti-substitution a weak clustering of the paramagnetic Mn^{4+} ions in the octahedral sites was described, in contrast to Mg substitution, where long-range ordering is present for all compositions.

Recently,[16] we described a two-phase mechanism and studied the changes in X-ray-determined lattice parameters during 5-V lithium deintercalation from $LiNi_{0.5}Mn_{1.5}O_4$. The lithium local environment during charging has been studied in detail by ^{6}Li MAS NMR.[21] However, to our knowledge no study on the evolution of the local structure around Mn^{4+} with lithium extraction has been carried out. This will be carried out here by using EPR spectroscopy. EPR technique has been shown to give valuable information on the electronic structure and cationic distribution in manganese spinels containing Mn^{4+} only (such as $LiLi_{1/3}Mn_{5/3}O_4$ [22] and $LiCoMnO_4$ [23]) and mixed Mn^{3+}/Mn^{4+} ions ($Li_{1+x}Mn_{2-x}O_4$ [24,25] and $LiCo_xMn_{2-x}O_4$ [26,27]). A second aim of this work is to evaluate the role of a large-extent substitution of a nonactive element such as magnesium at different Ni/Mg ratios, during the charge and discharge of the test cells.

Experimental Section

A precursor method was used to obtain $LiMg_yNi_{0.5-y}Mn_{1.5}O_4$ ($x = 0$, 0.25, 0.5) compounds. Thus, low crystalline oxyhydroxide was precipitated from a solution in a 3:2 water/ethanol mixture of $Ni(NO_3)_2{\cdot}6H_2O$, $Mg(NO_3)_2{\cdot}6H_2O$, and $Mn(NO_3)_2{\cdot}4H_2O$, by addition of a $LiOH{\cdot}H_2O$ solution with a 10% Li-excess. The slurry was stirred and heated in air to dryness. The fine powdered solid was further annealed at 400 °C under an air atmosphere. The low-crystallinity product was ground in an agate mortar and reannealed at 800 °C for 1 day in an air atmosphere. $LiNi_{0.5}Mn_{1.5}O_4$ samples for neutron diffraction recordings were obtained as described in ref 9, with annealing at 700 and 800 °C during 5 days in both cases. All samples were slowly cooled to the room temperature at 0.8 °C per minute.

X-ray powder diffraction (XRD) patterns were recorded on a Siemens D5000 instrument, using Cu Kα radiation and a graphite monochromator. The unit cell parameters are obtained from least-squares fitting of all peak positions ($10° \leq 2\theta \leq 90°$). The electrodes for ex-situ XRD were always prepared inside the glovebox, by carefully opening the cells, placing the products on a glass sample holder, and covering them with a plastic film to avoid exposure to air. Neutron diffraction (ND) experiments were carried out at room temperature on the high-resolution D1A diffractometer of the Institute Laue-Langevin (ILL, Grenoble, France) with wavelength 1.91140 Å, step 0.050 (°, 2-θ), and data acquisition time of 4 h by each sample. Fourier transform IR spectroscopy (FTIR) was carried out with a Bomem MB-100 spectrometer, using KBr pellets.

The EPR spectra were recorded as a first derivative of the absorption signal of an ERS-220/Q (ex-GDR) spectrometer within the temperature range of 90−400 K. The g factors were determined with respect to a Mn^{2+}/ZnS standard. The signal intensity was established by double integration of the experimental EPR spectrum. The analytical amount of Mn^{4+} was determined relative to a Li_2MnO_3 standard. For EPR measurements of positive electrode materials, the samples were manipulated in a glovebox in an Ar atmosphere. The lithium content of the charged/discharged compositions was calculated assuming that no current was consumed in side reactions, thus the charge/discharge level is overestimated.

The electrochemical behavior was tested using two-electrode Swagelok cells of the type $Li|LiPF_6(EC:DEC)|LiMg_yNi_{0.5-y}Mn_{1.5}O_4$. The electrodes were prepared as 7-mm-diameter pellets by pressing a mixture of 86% of the active oxide, 6% of PVDF binder, 4% Graphite (Merck), and 4% carbon black 4N (Strem) to improve the mechanical and electronic conduction properties, respectively. Lithium electrodes consisted of a clean 7-mm-diameter lithium metal disk. The commercial electrolyte solution (Merck LP40, 1 M $LiPF_6$ in a 1:1 w/w mixture of ethylene carbonate (EC) and diethyl carbonate (DEC)) was supported by porous glass-paper disks (Whatman). The electrochemical curves were carried using a multichannel MacPile II system. Potentiostatic cycling was performed at 10 mV/0.1 h rate and galvanostatic experiments at C/20, i.e., extraction of 1 Li/formula in 20 h.

Results and Discussion

Three different $LiMg_yNi_{0.5-y}Mn_{1.5}O_4$ compositions were obtained with $y = 0$, 0.25, and 0.5. The XRD pattern of $LiNi_{0.5}Mn_{1.5}O_4$ and $LiMg_{0.25}Ni_{0.25}Mn_{1.5}O_4$ samples could be indexed in the $Fd3m$ space group corresponding to a high-purity spinel phase (Figure 1a). In the cubic spinel notation, the lattice constant increases with the Mg amount: $a = 8.1530 \pm 0.0010$ Å; $a = 8.1798 \pm 0.0004$ Å, and $a = 8.1927 \pm 0.0005$ Å for $y = 0$, 0.25, and 1.0, respectively. For $LiMg_{0.5}Mn_{1.5}O_4$, new reflections occur, which are ascribable to a $P4_332$ superstructure by Mg and Mn ordering in 16d sites of the initial $Fd3m$ structure, as described in the literature.[4,6,7] The extent of metal ordering in the end members was also examined as a function of preparation temperature. For $LiMg_{0.5}Mn_{1.5}O_4$, significant changes are visible in the X-ray diffraction patterns obtained for samples annealed between 400 and 800 °C (Figure 1). On increasing preparation temperature up to 750 °C, an increase in the intensity of the superstructure lines is observed, but the changes are less notorious from 750 to 800 °C. Because of the similar X-ray scattering factors of Mn and Ni, the study for the $LiNi_{0.5}Mn_{1.5}O_4$ sample was

(13) Ariyoshi, K.; Yamamoto, S.; Ohzuku, T. *J. Power Sources* **2003**, *119−121*, 959.
(14) Zhong, Q.; Bonakdarpour, A.; Zhang, M.; Gao, Y.; Dahn, J. R. *J. Electrochem. Soc.* **1997**, *144*, 205.
(15) Amine, K.; Tukamoto, H.; Yasuda, H.; Fujita, Y. *J. Power Sources* **1997**, *68*, 604.
(16) Alcántara, R.; Jaraba, M.; Lavela, P.; Tirado, J. L. *Electrochim. Acta* **2002**, *47*, 1829.
(17) Zhecheva, E.; Stoyanova, R.; Alcántara, R.; Lavela, P.; Tirado, J. L. *Pure Appl. Chem.* **2002**, *74*, 1885−1894.
(18) Myung, S.-T.; Komaba, S.; Kumagai, N.; Yashiro, H.; Chung, H.-T.; Cho, T.-H. *Electrochim. Acta* **2002**, *47*, 2543.
(19) Takahashi, K.; Saitoh, M.; Sano, M.; Fujita, M.; Kifunec, K. *J. Electrochem. Soc.* **2004**, *151*, A173.
(20) Ariyoshi, K.; Iwakoshi, Y.; Nakayama, N.; Ohzuku, T. *J. Electrochem. Soc.* **2004**, *151*, A296.
(21) Lee, Y.-J.; Eng, C.; Grey, C. P. *J. Electrochem. Soc.* **2001**, *148*, A249.
(22) Stoyanova, R.; Gorova, M.; Zhecheva, E. *J. Phys. Chem. Solids* **2000**, *61*, 615.
(23) Stoyanova, R.; Zhecheva, E.; Gorova, M. *J. Mater. Chem.* **2000**, *10*, 1377.
(24) Massarotti, V.; Capsoni, D.; Bini, M.; Azzoni, C. B. *J. Solid State Chem.* **1997**, *128*, 80.
(25) Stoyanova, R.; Gorova, M.; Zhecheva, E. *J. Phys. Chem. Solids* **2000**, *61*, 609.
(26) Zhecheva, E.; Stoyanova, R.; Gorova, M.; Lavela, P.; Tirado, J. L. *Solid State Ionics* **2001**, *140*, 19.
(27) Mandal, S.; Rojas, R. M.; Amarilla, J. M.; Calle, P.; Kosova, N. V.; Anufrienko, V. F.; Rojo, J. M. *Chem. Mater.* **2002**, *14*, 1598.

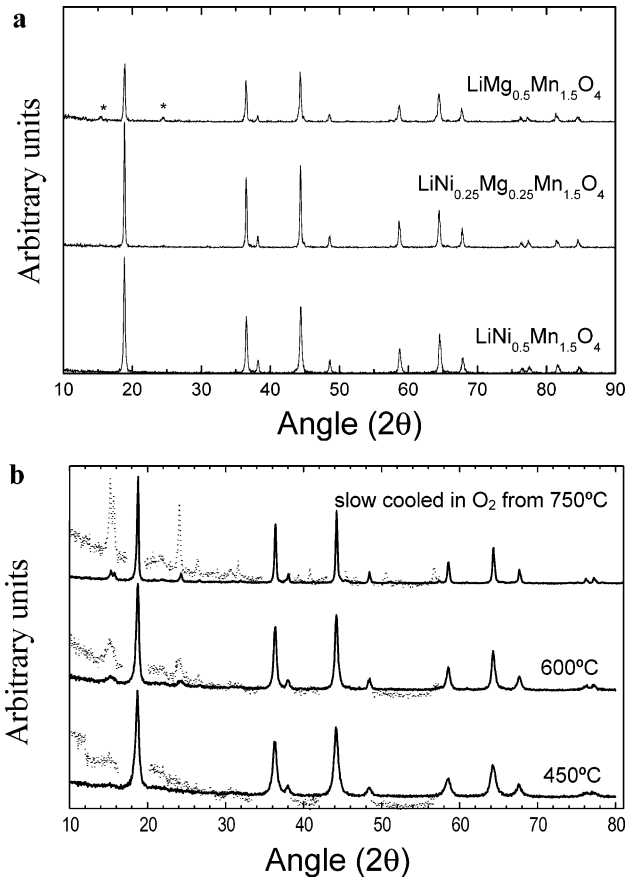

Figure 1. XRD pattern of (a) $LiMg_yNi_{0.5-y}Mn_{1.5}O_4$ series (y = 0, 0.25, and 0.5) obtained at 800 °C and (b) $LiMg_{0.5}Mn_{1.5}O_4$ obtained at different conditions. Dotted lines correspond to the superstructure $P4_332$ diffraction peaks.

carried out by using neutron diffraction (Figure 2). In this case, a decrease in the intensity and an increase in line broadening of the superstructure lines are observed on increasing preparation temperature from 700 to 800 °C. Thus, annealing conditions, as well as the presence of other elements such as Ti, influence the development of ordering in these systems.[4,8,9]

Since the early studies by Preudhomme,[2] infrared spectroscopy has proven to be a useful tool to qualitatively resolve cation ordering in $LiM_{0.5}Mn_{1.5}O_4$. In fact, the complexity of the IR spectra were used to detect ordering for both M = Ni and Mg in this pioneering study, and a disordered variant with less complex IR spectrum was also described for $LiNi_{0.5}Mn_{1.5}O_4$. More recently, we have shown how annealing temperature has a direct effect on the resolution of cation ordering bands in the IR spectra of $LiMg_{0.5}Mn_{1.5}O_4$.[17] Thus, for preparation temperatures between 450 and 750 °C the resolution of the spectra increases dramatically. On the other hand, the effect of composition on the FTIR spectra is summarized in Figure 3. Mg substitution leads to negligible shifts of the band frequencies. This fact arises from the similar ionic radius of Mg^{2+} (72 pm) and Ni^{2+} (69 pm), with a similar strength of the M−O bonding. The ordering bands are resolved for the three compositions. This is in agreement with XRD of $LiMg_{0.5}Mn_{1.5}O_4$ and ND of $LiNi_{0.5}Mn_{1.5}O_4$. Moreover it is also indicative that the ordering is also present in the intermediate composition. The influence of the annealing conditions on the FTIR spectra fine structure of $LiNi_{0.5}Mn_{1.5}O_4$ samples was also previously reported.[28] In this paper, the lack of 4-V plateau and hence of Mn^{3+} in the pristine spinel was correlated to the presence of absorption bands with a well-resolved fine structure.

To assess the local ordering in these spinels EPR studies were carried out on the different compositions. The $LiNi_{0.5}Mn_{1.5}O_4$ compound shows a ferrimagnetic order in the spinel structure below T_N = 130 K.[1,8] For 1:3 cation ordering in the octahedral spinel sublattice, every 4b octahedron occupied by Ni^{2+} is surrounded by six 12d octahedra containing Mn^{4+} only, while 4 Mn^{4+} and 2 Ni^{2+} form the first metal shell of Mn^{4+} occupying 12 d sites. As a result, the ferrimagnetic behavior is a result from 90° ferromagnetic $Mn^{4+}-O^{2-}-Mn^{4+}$ and $Ni^{2+}-O^{2-}-Ni^{2+}$ interactions and stronger 90° antiferromagnetic $Ni^{2+}-O^{2-}-Mn^{4+}$ interactions. Above the magnetic ordering temperature, some residual antiferromagnetic $Ni^{2+}-O^{2-}-Mn^{4+}$ correlations are preserved, culminating at $T > 450$ K in paramagnetic state.[1] The EPR spectrum of $LiNi_{0.5}Mn_{1.5}O_4$, collected between 140 and 410 K where the Curie−Weiss law is not obeyed, consists of resonance absorption characterized with Lorentzian line shape (Figure 4). On cooling, there is a strong resonance shift, with the apparent g-factor being changed from 2.022 to 1.946 (Figure 5). In the same temperature range, a line narrowing takes place (Figure 5). The signal disappears below 150 K. Thus, the EPR response from $LiNi_{0.5}Mn_{1.5}O_4$ can be associated with the residual antiferromagnetic correlations between Ni^{2+} and Mn^{4+} ions.

To rationalize the observation of the resonance absorption for $LiNi_{0.5}Mn_{1.5}O_4$, Figure 4 gives also the EPR spectra of two spinel compositions, $LiMg_{0.5}Mn_{1.5}O_4$, and $LiNi_{0.25}Mg_{0.25}Mn_{1.5}O_4$, in which the diamagnetic Mg^{2+} ions and mixed Mg^{2+}/Ni^{2+} ions substitute for paramagnetic Ni^{2+} ions. $LiMg_{0.5}Mn_{1.5}O_4$ displays ferromagnetic order at T_c = 38 K due to 90° ferromagnetic $Mn^{4+}-O^{2-}-Mn^{4+}$ interactions.[1,8] In this case, a single Lorentzian line accounts for the EPR spectrum of $LiMg_{0.5}Mn_{1.5}O_4$. The resonance absorption remains constant between 100 and 410 K, with the g-factor being 2.015. The ferromagnetic interactions between Mn^{4+} ions determine the line narrowing on cooling. The EPR parameters observed for $LiMg_{0.5}Mn_{1.5}O_4$ spinels are typical for ferromagnetically coupled Mn^{4+} ions at temperatures higher than that of the magnetic order. When mixed Ni^{2+}/Mg^{2+} ions substitute for paramagnetic Ni^{2+}, the EPR response for $LiMg_{0.25}Ni_{0.25}Mn_{1.5}O_4$ is similar to that for $LiNi_{0.5}Mn_{1.5}O_4$ in terms of line narrowing and resonance shift with the recording temperature. Close inspection of Figure 5 shows that the apparent g-factor is more sensitive toward the magnetic dilution of the Ni^{2+} sublattice by Mg^{2+} or Mg^{2+}/Ni^{2+}, whereas the line width undergoes less obvious changes. On the other hand, this result means that bivalent cations (paramagnetic Ni^{2+} and diamagnetic Mg^{2+}) are statistically distributed over 4b sites without perturbing the total 1:3 M^{2+}/Mn^{4+} ordering in the octahedral spinel sublattice.

The potentiostatic charge and discharge in the range between 3.0 and 5.1 V of test lithium cells using the $LiMg_yNi_{0.5-y}Mn_{1.5}O_4$ series are given in Figure 6a. As one can see, $LiNi_{0.5}Mn_{1.5}O_4$ shows only one oxidation

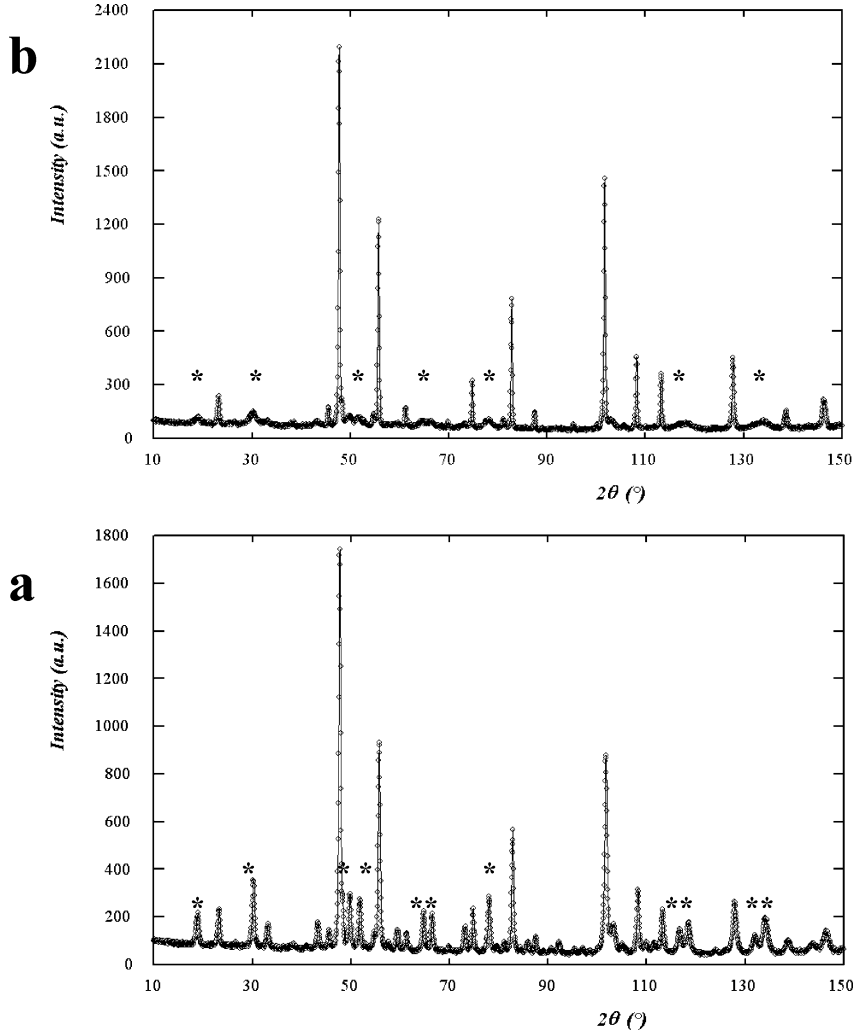

Figure 2. Neutron diffraction patterns of $LiNi_{0.5}Mn_{1.5}O_4$ samples obtained at 700 °C (a) and at 800 °C (b). Signals corresponding to a superstructure are marked.

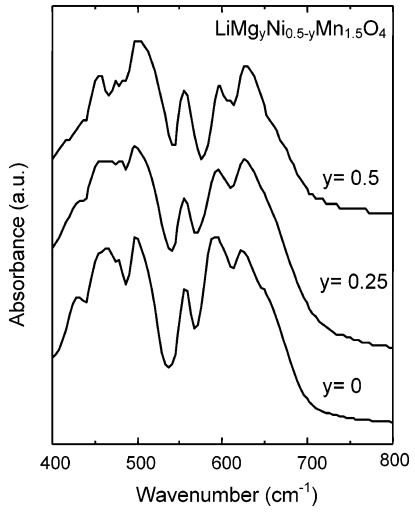

Figure 3. FTIR spectra of $LiMg_yNi_{0.5-y}Mn_{1.5}O_4$ series ($y = 0$, 0.25, and 0.5).

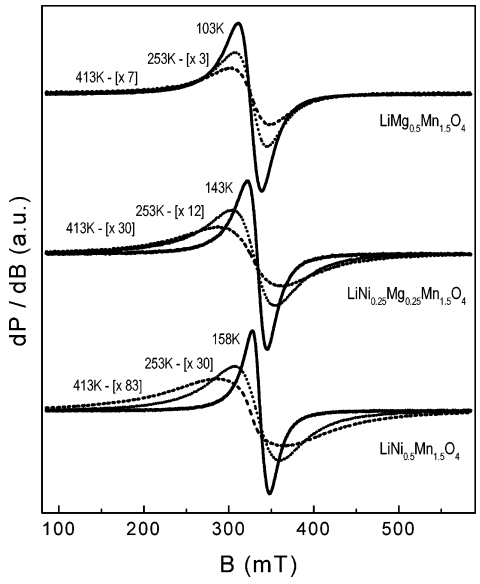

Figure 4. EPR spectra of $LiNi_{0.5}Mn_{1.5}O_4$, $LiNi_{0.25}Mg_{0.25}Mn_{1.5}O_4$, and $LiMg_{0.5}Mn_{1.5}O_4$ collected at different recording temperatures: 413 K (dashed lines); 293 K (dotted lines); and $T < 160$ K (full lines). The intensification of the spectrum is shown in brackets.

peak together with the reduction peak in the high-voltage region. These peaks have been ascribed to Li extraction/insertion from/into $LiNi_{0.5}Mn_{1.5}O_4$ involving the Ni^{2+}/Ni^{4+} oxidation/reduction reaction.[14,28] By increasing the Mg content, the high-voltage plateau disappears. In addition, no electrochemical activity is

(28) Ohzuku, T.; Ariyoshi, K.; Yamamoto, S.; Makimura, Y. *Chem. Lett.* **2001**, 1270.

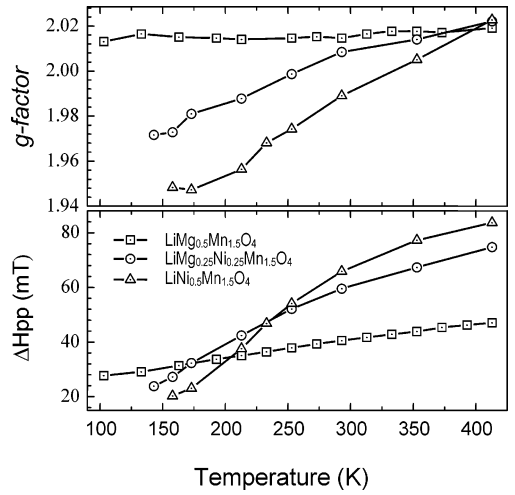

Figure 5. Temperature dependence of the apparent *g*-factor and the line width for $LiNi_{0.5}Mn_{1.5}O_4$, $LiNi_{0.25}Mg_{0.25}Mn_{1.5}O_4$, and $LiMg_{0.5}Mn_{1.5}O_4$.

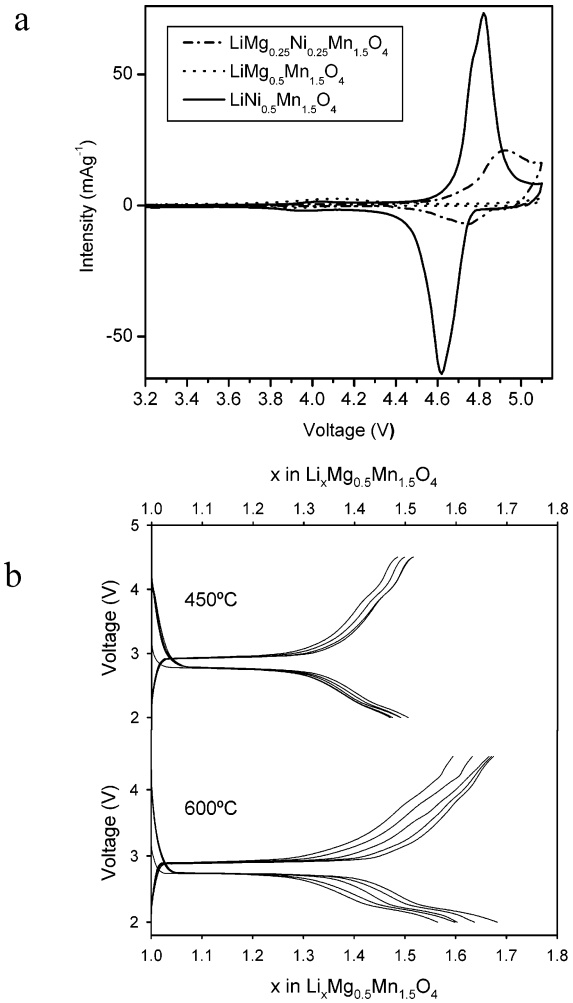

Figure 6. (a) Potentiostatic curves of $LiMg_yNi_{0.5-y}Mn_{1.5}O_4$ series (y = 0, 0.25, and 0.5) obtained at 10 mV/0.1 h. (b) Galvanostatic curves of $Li_xMg_{0.5}Mn_{1.5}O_4$ annealed at 450 and 600 °C in the 3-V region.

observed in the 4-V region, indicating the negligible presence of Mn^{3+} in the spinel composition. Although this situation is predicted by the nominal stoichiometry, the presence of trivalent manganese is commonly found when the annealing temperatures are high and cause the loss of oxygen.[14] It demonstrates that a slow cooling process after annealing also favors the Mn^{3+} oxidation process. Moreover, the lack of oxidation signal in the 5-V region evidences that the Mn^{4+} ions are not electroactive in this region, as found in related spinels.[29]

Galvanostatic cycling experiments of $LiMg_{0.5}Mn_{1.5}O_4$ obtained at 450 and 600 °C in the 2.0−4.5-V cell potential window are shown in Figure 6b. Whereas $LiNi_{0.5}Mn_{1.5}O_4$ displays a single plateau in the 3-V region,[10,12] three well-resolved reactions appeared for $LiMg_{0.5}Mn_{1.5}O_4$.[30] A plateau at ca. 2.8 V was the main feature in Figure 6b for both preparation temperatures. The nature of this effect has been widely studied in $LiMn_2O_4$. The reversible process is unambiguously attributed to Li insertion in 16c octahedral sites of the spinel structure. No clear differences are detected for both samples at this cell potential, with the exception of a more reduced capacity for the oxide obtained at the lower temperature. For lower voltages, $LiMg_{0.5}Mn_{1.5}O_4$ obtained at 600 °C shows a well-resolved reduction plateau at 2.2 V. The observation of weak reduction steps below 2.2 V has been already reported for the ordered modification of $LiMg_{0.5}Mn_{1.5}O_4$, and they have been related with the cubic−tetragonal transition for $Li_{1+x}Mg_{0.5}Mn_{1.5}O_4$.[30] For higher voltages, a low extension plateau at 4 V is detected, more clearly for the spinel obtained at 450 °C. The lower synthesis temperature may condition an incomplete manganese oxidation. The remaining Mn^{3+} is reversibly oxidized but with a very limited contribution to specific capacity. The lower capacity of the disordered spinel oxide can be attributed to a wider exchange of ions from their normal sites with the possible existence of Mg atoms in Li sites or octahedral empty sites. This fact would impede the optimal alkaline ions' occupancy and mobility in the spinel framework.

To study the local coordination of Mn^{4+} during lithium extraction/insertion in these positive electrode materials, the $LiNi_{0.5}Mn_{1.5}O_4$ spinel was selected, due to its better performance in the high-voltage range. Figure 7 compares the EPR spectra of $LiNi_{0.5}Mn_{1.5}O_4$ spinels after lithium extraction and consecutive Li reinsertion. The strong resonance absorption is still observed for the samples with 30 and 70% of extracted lithium. Moreover, the apparent *g*-factor displays the same temperature dependence in the range 140−293 K as in the case of initial composition, whereas the line width is slightly higher for the samples with 70% of extracted lithium (Figure 8). Below 140 K, there is a resonance shift in opposite direction for the latter sample only, and the line width increases suggesting a magnetic disorder. The resonance absorption disappears at 113 K (Figures 7b and 8a).

The electrochemical extraction of Li has been shown to proceed simultaneously with the oxidation of paramagnetic Ni^{2+} to diamagnetic Ni^{4+}. However, EPR spectroscopy shows that Ni^{2+}−Mn^{4+} spin system at $LiNi_{0.5}Mn_{1.5}O_4$ is preserved up to 70% of Li extraction. The EPR intensity is reduced following the changes in the Li amount: from I = 1.0 to 0.67 and 0.17 for initial and after 30 and 70% of extracted lithium, respectively.

(29) Wang, X.; Iltchev, N.; Nakamura, H.; Noguchi, H.; Yoshio, M. *Electrochem. Solid-State Lett.* **2003**, *6*, A99.
(30) Le Cras, F.; Bloch, D.; Anne, M.; Strobel, P. *Solid State Ionics* **1996**, *89*, 203.

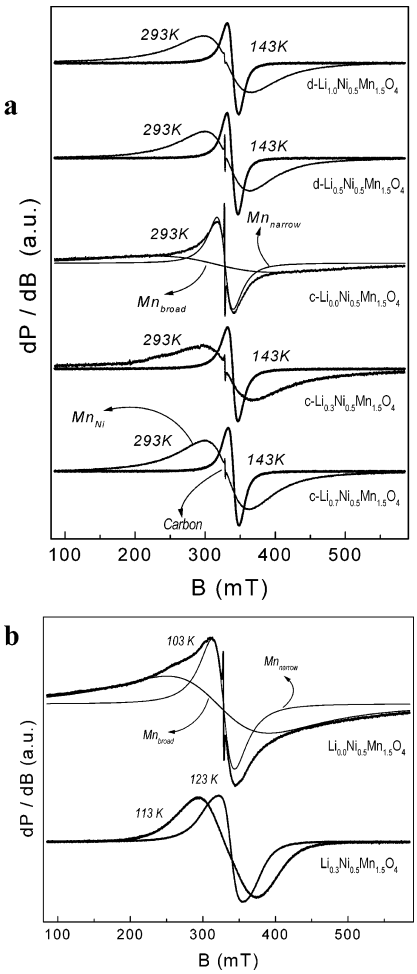

Figure 7. (a) EPR spectra of $Li_xNi_{0.5}Mn_{1.5}O_4$ after first charge to 5.1 V and subsequent discharge to 3.0 V. The signals coming from Mn and Ni coupled spins (Mn_{Ni}), localized Mn^{4+} ions in contracted spinel cell (Mn_{narrow}), and localized Mn^{4+} ions in extended spinel cell (Mn_{broad}) are indicated. The signal from carbon mixture is also shown. (b) EPR spectra, recorded at temperatures lower than 143 K, of $Li_{0.3}Ni_{0.5}Mn_{1.5}O_4$ and $Li_{0.0}$-$Ni_{0.5}Mn_{1.5}O_4$.

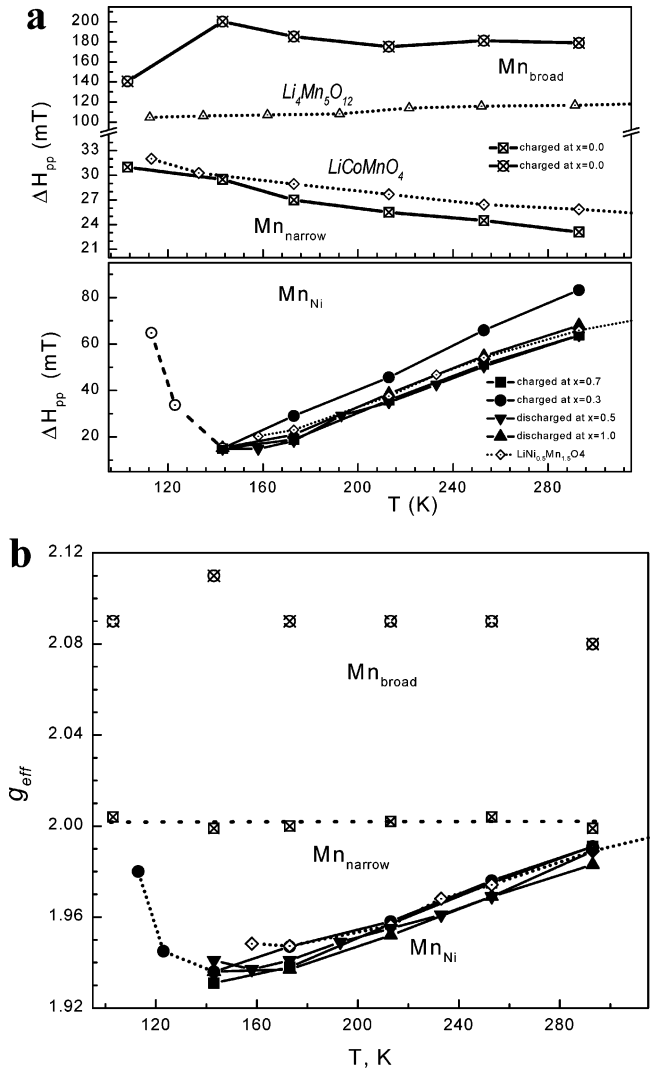

Figure 8. (a) Temperature dependence of the EPR line width of signals from Mn and Ni coupled spins (Mn_{Ni}), localized Mn^{4+} ions in contracted spinel cell (Mn_{narrow}), and localized Mn^{4+} ions in extended spinel cell (Mn_{broad}) for $LiNi_{0.5}Mn_{1.5}O_4$ after first charge and subsequent discharge. For the sake of comparison, the temperature variation of the EPR line width for $LiCoMnO_4$ and $Li_4Mn_5O_{12}$ compositions is also given. (b) Temperature dependence of the apparent *g*-factor of signals Mn_{Ni}, Mn_{narrow}, and Mn_{broad} for $LiNi_{0.5}Mn_{1.5}O_4$ after first charge and subsequent discharge.

The result obtained implies that the electrochemical extraction of Li from $LiNi_{0.5}Mn_{1.5}O_4$ can be regarded as a two-phase reaction including the initial composition and a new phase, which is EPR undetectable. This can be explained by the sensitivity of the EPR spectroscopy toward magnetically correlated spins as compared to localized spins. As an example, at 293 K the relative intensity of the resonance absorption of $LiNi_{0.5}Mn_{1.5}O_4$ is about 10 times higher than that for the signal due to localized Mn^{4+} in $LiMg_{0.5}Mn_{1.5}O_4$. In addition, it is interesting to compare the EPR behavior of $LiNi_{0.5}$-$Mn_{1.5}O_4$ during Li extraction with the ^6Li NMR experiments for charged $LiNi_{0.5}Mn_{1.5}O_4$ electrodes.[21] On the basis of NMR experiments, it has been shown that the charging process (up to 90% of extraction of Li) involves the Li removal without changes in the Li local environment. On the other hand, it appears that both EPR and NMR results give a complementary perspective to the ex-situ XRD experiments, where only one cubic phase is detected up to 50%[16] or 80%[18] of extracted Li. The changes in the local structure start with the charge process generating domains of localized spins. Only after sufficient extension of this phenomenon, may the domains coalesce to give a second X-ray detectable phase.[16,18,20,34]

The $Li_{0.0}Ni_{0.5}Mn_{1.5}O_4$ composition displays a completely different EPR spectrum. In this case, two signals can be resolved: at 293 K, the narrow signal with a Lorentzian shape (Mn_{narrow}) dominates the EPR spectrum of $Li_{0.0}Ni_{0.5}Mn_{1.5}O_4$, whereas the broader symmetrical signal (Mn_{broad}) is better visible on cooling. The intensity of the broader signal is about 10 times higher than that of the narrower. The important difference

(31) Masquelier, C.; Tabuchi, M.; Ado, K.; Kanno, R.; Kobayashi, Y.; Maki, Y.; Nakamura, O.; Goodenough, J. B. *J. Solid State Chem.* **1996**, *123*, 255.
(32) Greedan, J. E.; Raju, N. P.; Wills, A. S.; Morin, C.; Shaw, S. M.; Reimers, J. N. *Chem. Mater.* **1998**, *10*, 3058.
(33) Gee, B.; Horne, C. R.; Cairns, E. J.; Reimer, J. *J. Phys. Chem. B* **1998**, *102*, 10142.
(34) Mohamedi, M.; Makino, M.; Dokko, K.; Itoh, T.; Uchida, I. *Electrochim. Acta* **2002**, *48*, 79.

between two signals and the resonance absorption observed for $LiNi_{0.5}Mn_{1.5}O_4$ is the constancy of the *g*-factor in the temperature range 103−293 K: $g = 2.002$ and $g = 2.09$, for the narrower and broader signals, respectively. The line width for the narrow signal increases on cooling, while the broader signal is slightly narrowed below 173 K.

For the sample with an effective composition $Li_{0.0}Ni_{0.5}Mn_{1.5}O_4$, two EPR signals from localized Mn^{4+} ions are observed, indicating an exhaustion of paramagnetic Ni^{2+} ions in the vicinity of Mn^{4+} (Figures 7 and 8). However, the EPR spectrum of the "fully delithiated" oxide is different from that for $LiMg_{0.5}Mn_{1.5}O_4$. This can be understood if we consider the dependence of the magnetic $Mn^{4+}-Mn^{4+}$ interactions on the distance. The magnetic behavior of the manganese spinel is a result from the competition between 90° direct $Mn^{4+}-Mn^{4+}$ antiferromagnetic and 90° superexchange $Mn^{4+}-O^{2-}-Mn^{4+}$ ferromagnetic interactions.[31,1] Thus, it has been shown that superexchange ferromagnetic interactions dominate for $LiMg_{0.5}Mn_{1.5}O_4$ where the Mn−Mn contact is between 2.867(4) and 2.923(4) Å,[8] whereas an antiferromagnetic character is reported for both λ-MnO_2 and $LiCoMnO_4$ with $r_{Mn-Mn} = 2.84$ and 2.85 Å, respectively.[32,33] $Li[Li_{1/3}Mn_{5/3}]O_4$ composition having $r_{Mn-Mn} = 2.87$ Å is near the crossover between the ferromagnetic and antiferromagnetic transition.[31] The development of ferro- or antiferromagnetic interactions has an effect on the temperature variation of the EPR line width. The EPR line width decreases on cooling for ferromagnetically coupled Mn^{4+}, whereas for antiferromagnetically coupled Mn^{4+} there is an increase of the EPR line width. For the sake of comparison, Figure 8 gives the variation of the line width for Mn^{4+} containing spinels, $Li[CoMn]O_4$ and $Li[Li_{1/3}Mn_{5/3}]O_4$.[23,22] On the basis of this comparison, one may suggest that the narrow signal corresponds to an antiferromagnetic spinel phase with a contracted lattice constant ($r_{Mn-Mn} \approx 2.85$ Å or $a \approx 8.05$ Å), whereas the spinel phase with the expanded lattice constant ($r_{Mn-Mn} \approx 2.87$ or $a \approx 8.13$ Å) is responsible for the appearance of the broader signal. This result is in good agreement with the ex-situ XRD data on the changes of the lattice constant of $LiNi_{0.5}Mn_{1.5}O_4$ during electrochemical extraction of Li.[16,18,20]

Li reinsertion causes a recovering of the EPR behavior of the initial composition in terms of the temperature dependence of the apparent *g*-factor and the line width (Figures 7 and 8). This result reveals the good reversibility of the charging/discharging process for $LiNi_{0.5}Mn_{1.5}O_4$ spinel.

Conclusions

As found in the literature for some compositions in the $LiMg_yNi_{0.5-y}Mn_{1.5}O_4$ series, structural information obtained from XRD and/or neutron diffraction, as well as FTIR spectroscopy, reveals the occurrence of cation ordering in the octahedral sites, leading to a $P4_332$ space group superstructure. The results in this work show that the annealing temperature conditions the occurrence of the ordered variants in a different direction depending on the magnesium content. Thus, for $y \geq 0.25$ the superstructure lines become more clearly visible when the annealing temperature increases from 450 to 750 °C. In contrast, neutron diffraction patterns for $LiNi_{0.5}Mn_{1.5}O_4$ obtained at 700 and 800 °C evidenced the progressive loss of ordering when preparation temperature increases. This effect can be related with the formation of $Li_xNi_{1-x}O$ and Mn^{4+} reduction during annealing at 800 °C, which is less marked for the Mg-containing spinels. However, the electrochemical behavior in the high voltage region was hindered by the presence of large amounts non-oxidizing Mg^{2+} ions. Nevertheless, cycling in the 3-V region, which implies the Li insertion in octahedral sites (16d) along with Mn^{4+} reduction to Mn^{3+}, leads to an extended plateau in which capacity increased with annealing temperature for $LiMg_{0.5}Mn_{1.5}O_4$ samples.

The EPR spectrum of $LiMg_{0.5}Mn_{1.5}O_4$ consists of a single Lorentzian line due to ferromagnetically coupled Mn^{4+}. When diamagnetic Mg^{2+} is replaced by paramagnetic Ni^{2+}, the EPR response from residual antiferromagnetic correlations between Ni^{2+} and Mn^{4+} ions is observed for $LiMg_yNi_{0.5-y}Mn_{1.5}O_4$ compositions. This EPR behavior enables examination of the electronic structure $LiNi_{0.5}Mn_{1.5}O_4$ during the electrochemical extraction of Li in the 5-V region. Lithium extraction from $LiNi_{0.5}Mn_{1.5}O_4$ leads to an intensity loss in the EPR signal as a consequence of the oxidation of paramagnetic Ni^{2+} to diamagnetic Ni^{4+} without significant changes in local environment of Mn^{4+}. Fully delithiated $LiNi_{0.5}Mn_{1.5}O_4$ shows an EPR spectrum resulting from localized Mn^{4+} ions, indicating an exhaustion of paramagnetic Ni^{2+} ions in the vicinity of Mn^{4+} ions. The spectrum differs from that of $LiMg_{0.5}Mn_{1.5}O_4$, although in this case it can also be ascribed to Mn^{4+} ions. The predominance of superexchange ferromagnetic interactions in the latter oxide would justify the different profiles. Li reinsertion in $LiNi_{0.5}Mn_{1.5}O_4$ shows a good recovering of the initial properties making evident the notorious reversibility of this positive electrode material.

Acknowledgment. E.Zh. and R.S. are indebted to the National Science Fund of Bulgaria (Contract Ch1304/2003) for financial support. We acknowledge financial support from MCyT (contract MAT2002-00434) and Programa Ramón y Cajal. We also thank the Institute Laue-Langevin (Grenoble) for use of their neutron diffraction facilities.

CM035369C